2014 5th IEEE RAS & EMBS International Conference on
Biomedical Robotics and Biomechatronics (BioRob)
August 12-15, 2014. São Paulo, Brazil

A proposal to monitor muscle contraction through the change of electrical impedance inside a muscle

Olavo L. Silva[a], Thais H.S. Sousa[a], Isadora O. Hoffman[a],
Erick D.L.B. de Camargo[a], Fernando S. de Moura[a], Alessandro R.C. Martins[b],
Caio Biasi[b], Denise T. Fantoni[b] and Raul G. Lima[a]

Abstract— **Dynamically monitoring muscle contraction is an important task in sports training and rehabilitation programs. Internal muscles monitoring are specially challenging because they cannot be accessed by palpation or surface EMG. It is well known that blood flow through skeletal muscle can increase 15- to 25-fold during extreme exercise compared to its rest state. Additionally, at rest, some muscle capillaries have little or no blood flowing, but during strenuous exercise, all the capillaries open. With regard to electrical properties, blood resistivity is about half of muscle resistivity. Thus, global muscle resistivity have a tendency to change when it goes from rest to activity state. Recent results suggest that resistivity changes are related to contraction rate. Bearing that in mind, Electrical Impedance Tomography turns out to be an interesting signal to monitor muscle contraction by sensing resistivity changes related to muscle activity. If low intensity current is injected and electric potentials are measured through electrodes attached on skin, resistivity maps can be obtained using this data to solve an ill-posed inverse problem. In this work the electrical impedance was measured while a muscle was under repetitive contractions. Significant changes of electrical impedance were found in the frequency of contractions.**

I. INTRODUCTION

Robotic orthoses can be used as an assistive device for rehabilitation of subjects suffering neurological impairments such as spinal cord injuries and stroke. These orthoses serve as a torque generator substituting muscle's function. For this purpose, it is necessary the detection of the operator's intention to produce muscle torque. One way to accomplish this is using biological information such as the electrical properties of the skeletal muscle tissue, as the resistivity, that changes during the muscle contraction and that presents a different behavior when analyzed in the longitudinal and transversal directions, according to the muscle fiber direction. A promising technique to analyze the muscle resistivity is the Electrical Impedance Tomography (EIT) [1], [2], a non-invasive technique that can estimate the electrical resistivity distribution inside a domain. Thus, muscle resistivity would be an interesting signal to monitor in order to capture operator's intention to control a robotic orthosis.

Electrical properties of biological tissues have been extensively studied both *in vivo* and *in vitro* in a wide range of frequencies [3], [4], [5]. Table I presents resistivity and reactivity values for selected tissues found in musculo-skeletal system[1]. As can be seen, the resistivity difference can be as low as 5% comparing muscle and tendon or can be more than 100 times greater if bone marrow and muscle are compared.

At rest, blood flow through skeletal muscle averages from 3 to 4 ml/min/100g of muscle but during extreme exercise in a well-conditioned athlete, this can increase 15- to 25-fold, rising to 50 to 80 ml/min/100 g of muscle. Additionally, at rest, some muscle capillaries have little or no blood flowing, but during strenuous exercise, all the capillaries open [6, Ch.21]. Moreover, blood flow continuously oscillates at rest, as an effect of the heart beat and blood pressure. During exercise these oscillations are even more pronounced, being also influenced by the intramuscular pressure variations [7].

TABLE I
ELECTRICAL PROPERTIES OF TISSUES FROM THE MUSCULO-SKELETAL SYSTEM AT 125KHZ

Tissue	Resistivity (Ohm.m)	Relative Permitivity
Blood	1.41965	5076.00
Tendon	2.57202	406.60
Muscle	2.72405	7550.00
Blood vessel	3.13185	784.60
Cartilage	5.57414	2515.00
Nerve	11.83992	4238.00
Fat	40.86637	77.92
Bone cortical	47.93864	219.10
Bone marrow	295.68303	96.08

Skeletal muscle are known to suffer architectural changes under contraction. It shortens, its cross sectional area increases, its pennation angle varies [8] and even its volume may change. Despite the experiments of Jan Swammerdam, who demonstrated in 1663 the volume constancy of an isolated frog muscle [9, p.22], latter confirmed[2] by Baskin and Paolin [10], recent *in vivo* MRI studies suggest that

This work was supported by Capes, CNPq and Fapesp

[a] Mechanical Engineering, Polytechnic School, University of São Paulo, Brazil

[b] Faculty of Veterinary Medicine and Zootechnics, University of São Paulo, Brazil

[1]These data were taken from http://niremf.ifac.cnr.it/tissprop/, which is based on the parametric model and the parameter values developed by C. Gabriel and colleagues.

[2]Baskin and Paolini measured the volume of excised *Rana pipiens* gastrocnemius muscle inside a chamber at 24° C after a single rectangular pulse of 6V amplitude and 4 msec duration. They found a maximum volume variation of $5 \times 0.603 \cdot 10^{-5}$ cm^3/g for a 0.945 g weight muscle. Considering that muscle density is about 1.06 g/cm^3, the muscle of the experiment had approximately 0.891 cm^3. Thus, the Δ volume measured of $2.849 \cdot 10^{-5}$ cm^3 correspond to a percentage volume variation of 0.003%.

masticatory muscles volumes could change from 0.7% to 9.0% [11].

Ions are the principal charge carriers in biological tissues. In this situation electrical conductivity is thus determined by ion concentration, valence and ion mobility. During exercise several reactions involving the release and suppression of ions take part. The breakdown of phosphocreatine results in a rise in the inorganic phosphate concentration $[P_i]$. In skeletal muscle, resting $[P_i]$ is about 1–5 mM but can rise to 30–40 mM during intense exercise [12]. The glycogen-lactic acid system for the formation of ATP in the absence of oxygen may also interfere in the concentration of free H^+ inside muscle cells. There is a net balance of 2 H^+ if the glycolysis is started from glucose or 1 H^+ if it is started from glycogen [13]. Ca^+ also plays an important role in muscle cells. It initiates the actin-myosin coupling when it is released in large quantities from sarcoplasmic reticulum to the sarcolemma and it is pumped back into sarcoplasmic reticulum when action potential ceases. Moreover, high force contractions present in high intensity exercise may cause mechanical disruption of the sarcomeres and perhaps the sarcolemma membrane. The latter would lead to an influx of Ca^{+2} and the activation of cell proteases and phospholipase activity, which would further contribute to fiber degradation [14].

The belief that muscle electrical properties can carry on valuable clinical information is not new. Electrical Impedance Myography (EIM) is a non-invasive technique for the evaluation of neuromuscular disease that assess muscle resistance and reactance with the application and measurement of high-frequency, low-intensity electrical current, usually by a tetrapolar electrode system [15]. EIM has already been found a good correlation between decreasing phase ($\arctan(X/R)$) and increasing disease severity for a wide range of muscle shapes and neuromuscular diseases [16]. Shiffmann et al [17] measured with EIM the resistance and reactance of the finger flexor muscles under voluntary isometric contraction. Their equipment has a 800 μA, 50kHz current source connected to 2.8 $\times$ 2.9 cm electrodes placed on the abductor pollicis brevis and biceps brachii. They observed that changes in resistance R and reactance X are both positive in the isometric gripping force measurements.

The first studies about the impeditivity of biological tissues where performed in dead animals or *in vitro* [3]. These data are not adequate to the purposes of this work because does not reveal how factors that only exist in living tissues influence muscle impeditivity under contraction. Recently Ahad et al [18] measured the conductivity and relative permittivity in gastrocnemius muscle of immature and mature rats, however in this study, as well as in many others [19] the focus is the current frequency dependency over conductivity measurements. Some authors have made *in vivo* conductivity measurements of rat [20] and human [21] muscles at rest. There is one reported study [17] in which the impedance of the forearm flexor muscles were measured with EIM technique during isometric contractions. The results confirm that the resistance and reactance of the muscles increase when they exert gripping force via isometric contraction.

The authors have shown in [22] that resistivity changes in human soleus and tibialis anterior muscles could be detected in a non-invasive way using EIT. Fig. 1(b) show a difference image formed from two EIT images, one in ankle plantar flexion and the other in dorsi-flexion, during successive ankle flexion exercise with the knee flexed. Comparing Figs. 1(a) and 1(b) is possible to observe that a positive variation area (in red) is located close to soleus anatomical area and a negative variation (in blue) is located close to tibialis anterior area.

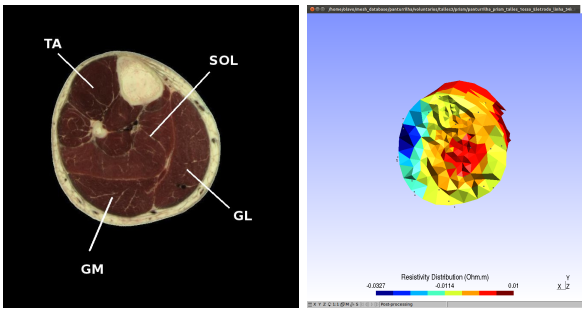

(a) Anatomical cross section. (b) Corresponding EIT image.

Fig. 1. Difference EIT image of human right calf between two moments: ankle plantar flexion and dorsi-flexion.

A. Objectives

The aim of this work is to present the physiological evidences that may help to explain resistivity variations observed in muscle EIT images. We present data that correlates muscle contraction and invasively measured muscle electrical impedance changes. Therefore, we suggest the use of electrical impedance changes observed in EIT images to monitor muscle contraction and the use of this estimate muscle contraction for controlling robotic orthoses.

II. METHODOLOGY

A. Stimulation protocol

Three male domestic swines, from 2 to 3–months old, weighing between 28 and 30 kg were selected for this experiment. They were adequately sedated according to the protocol approved by Comissão de Bioética da Faculdade de Medicina Veterinária e Zootecnia da Universidade de São Paulo. The swine was placed in dorsal decubitus and an incision was made to expose biceps brachii muscle and musculo-cutaneous nerve of the right limb. The probe was inserted transversely[3] to muscle fibers for impedance measurement. Two stimulation tweezers electrodes were attached to musculo-cutaneous nerve and connected to a neuromuscular electrotherapy device (*QUARK, model FES VIF 995, Piracicaba, Brasil*).

The equipment was set in *burst* mode where trains of pulses were delivered at a frequency of 2Hz, each pulse

[3]By transverse direction we understand that current flowing from needle 1 to needle 4 runs perpendicularly to muscle fibers and by longitudinal direction it runs parallel to muscle fibers.

with a period of $100\mu s$ with a frequency of 100Hz inside each train. Current intensity was adjusted to produce visually observable muscle fatigue.

Data collection was triggered with muscle initially at rest. After one minute, the electrotherapy device was turned on, with the right limb manually held to impose resistance. Stimulation was kept for one minute and then turned off. Data collection was maintained for additional four minutes, with muscle at rest and resumed for one more minute of stimulation. After the end of second stimulation, data collection was maintained for additional four minutes, totalizing 11 minutes of data collection. The experiment was repeated with the probe inserted longitudinally to fibers of the same right biceps brachii muscle.

B. Data acquisition system

The impedance measurement device is a system composed by a probe, a waveform generator (*Ultra Low Distortion Waveform Generator, Model DS-360; Stanford Research Systems, 1290-D Reamwood Ave., Sunnyvale, CA 94089*), a voltage to current converter and a ICS-645 Digital Aquisition Card (DAC) (*Interactive Circuits and Systems LTD, 5430 Canotek Rd, Gloucester ON, K1J 9G2, Canada*) connected to a computer. The probe is composed by four 0.7 mm diameter needles, disposed in a rectangular array of 12.2 mm length and 2.0 mm width Fig. II-B. The current source is controlled by the waveform generator to produce a sine wave at 125 kHz. The current amplitude is regulated in order not to saturate AD converters of ICS-645 card and typically varied from 1.0 to 3.0 mA. DAC sampling frequency was set to 2.5 MSps. It collects a set of 8000 samples per channel at every 0.10s, during a period of 11 minutes.

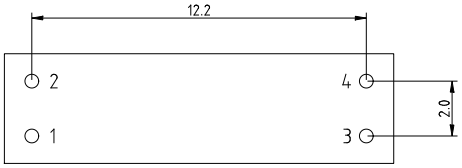

Fig. 2. Probe schematics

C. Signal filtering and demodulation

Sine signals from DAC were multiplied by a Hann window and then filtered with a passband filter from 115 to 135 kHz. Each set of 8000 points was fitted to Eq. 1, where $f = 125$kHz and A, B, C and Δf are unknowns.

$$f(t) = A\sin(2\pi t(f+\Delta f)) + B\cos(2\pi t(f+\Delta f)) + C \quad (1)$$

which is equivalent to

$$f(t) = \bar{A}\sin(2\pi t(f+\Delta f) + \phi) + \bar{C} \quad (2)$$

Once the coefficients A, B and C are found, its amplitude $\bar{A}$ and phase ϕ were computed. Current source is connected to needle 1 and a sentinel resistance ($R = 198.3\Omega$) is placed between needle 4 and ground. Since the phase of the current signal is assumed to be zero, the phase of channel 4 was subtracted from the phase of all channels. Therefore, the impedance of the tissue can be computed from needles 2 and 3 and the applied current is computed from needle 4 electric potential.

Admittivity was calculated with an approach presented in [23]. Briefly, one has to seek for an uniform admittivity distribution γ that satisfies generalized Laplace equation and known electric potentials at the needles. This problem can be solved using an Newton-Raphson algorithm and a finite element mesh.

III. RESULTS

Figure 3 presents the results of resistivity and reactivity in transversal direction. The timespan of the experiment can therefore be divided in five distinct periods: (a) rest, from 0 to 1 min; (b) 1st stimulus, from 1 to 2 min; (c) 1st recovery, from 2 to 6 min, (d) 2nd stimulus, from 6 to 7 min and (e) 2nd recovery, from 8 to 11 min. For experiment *Exp6-burst,left* the second stimulus was eliminated and the 1st recovery remained for 5 min.

It can be observed in Fig. 3 that there is a resistivity high frequency variation during the stimulation period (from minute one to two and from minute six to seven). Besides the high frequency variation, the average resistivity during the stimulus is higher then the muscle is not in activity. See, for example, experiment *Exp3-burst*, where this effect is more pronounced. During the recovery period (from minutes two to six) there is a slow decay trend of resistivity for experiments *Exp3-burst* and *Exp6-burst,left*, while for experiment *Exp4-burst* resistivity tend to rise.

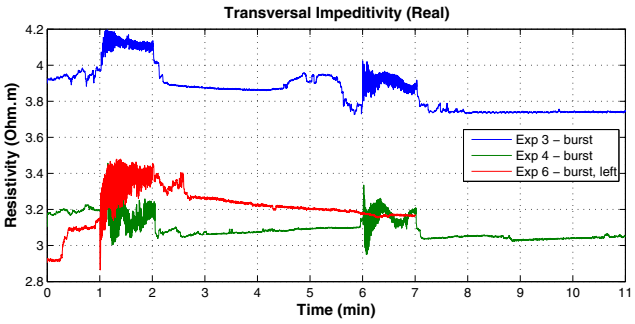

Fig. 3. Transversal resistivity of swine muscle.

In Figure 4, a short time Fourier transform (STFT) was performed over the resistivity curves presented in Figure 3. The FFT was performed over a window with 15.0 s length and it was swept in 0.5 s intervals. Frequency axis is plotted from $0.2 - 5.0$ Hz to hide low frequency artifacts of FFT. It is possible to observe that from 60 s to 120 s, the most intense spectrum component is around 2.0 Hz and the second one at 4.0 Hz. There is a considerable decay 25s after the beginning of stimulation coinciding with the decay of force production which was orally stated at the video recordings of the experiments. Although not continuously recorded, the swine heart rate was registered and varied

from 130 bps to 168 bps and from 168 bps to 27 bps during the 1st stimulus of experiment `Exp-3,burst` and `Exp-4,burst`, respectively.

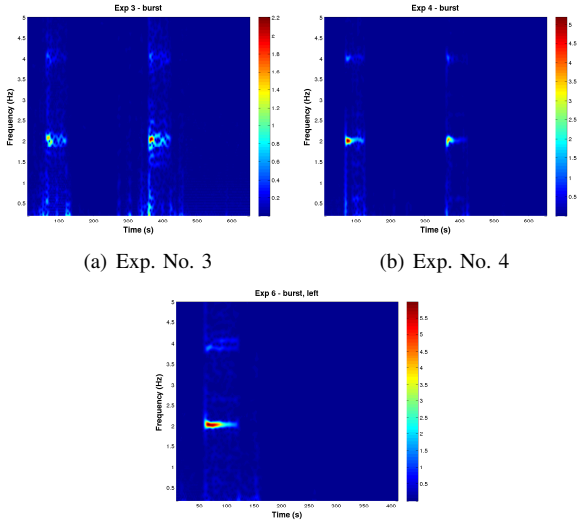

(a) Exp. No. 3 (b) Exp. No. 4

(c) Exp. No. 6

Fig. 4. Short-time FFT analysis of individual resistivity measurements of swine muscle in transversal direction.

Figure 5 presents the results of resistivity in longitudinal direction. For experiments `Exp6-burst,left` and `Exp6-burst,right`, which were performed at different limbs of the same animal, the second stimulus was eliminated and the first recovery remained for 5 min.

The high frequency variation was also observed in Figs. 5 for the longitudinal measurement of resistivity. However, the variability was smaller during the 2nd stimulus (minutes six to seven) of experiments `Exp3-burst` and `Exp4-burst`. It is also noticeable that resistivity decreases when the muscle is in activity which is exactly the opposite behavior found for transversal measurements. See, for example, experiment `Exp6-burst,right`, where this effect is more pronounced.

During the recovery period (from minutes two to six) the resistivity of all experiments tend to decay, except for `Exp3-burst`, which remain almost constant. It is important to stress that this is the same behavior found for transversal measurements.

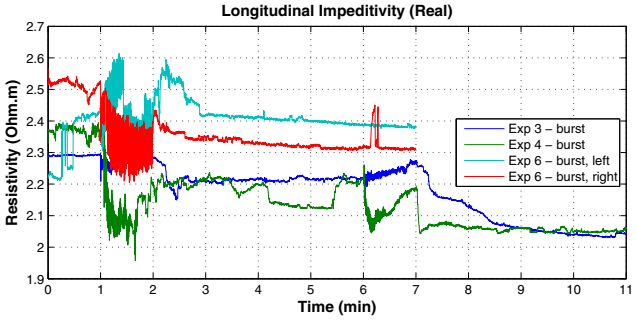

Fig. 5. Longitudinal impeditivity measurements of swine muscle.

Figure 6 shows the short time Fourier transform performed over the resistivity curves of Fig. 5 performed with the same parameters used in transversal measurements. Again it is possible to observe that the spectrum is more intense around 2.0 Hz. The the color scale limits of Fig. 6 indicate that the intensity of the signal at the frequency of contraction is from five to eight times higher than other frequencies. In Fig. 4 this ratio is about 10 times.

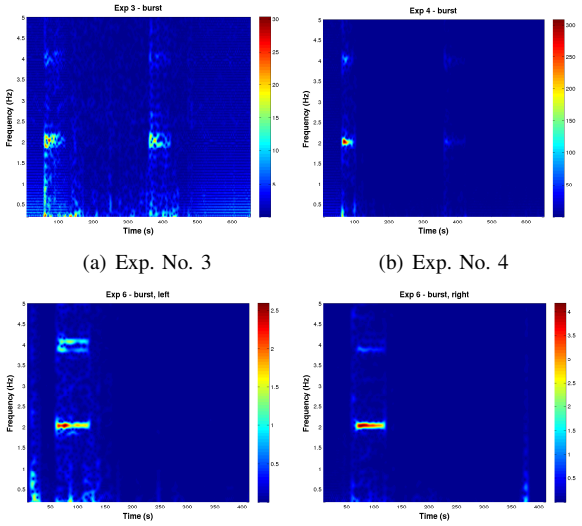

(a) Exp. No. 3 (b) Exp. No. 4

(c) Exp. No. 6, left limb (d) Exp. No. 6, right limb

Fig. 6. Short-time FFT analysis of individual impeditivity measurements of swine muscle in longitudinal direction.

IV. CONCLUSIONS

We have demonstrated some evidences that relate muscle activity and tissue resistivity changes. The contribution of this work is twofold: it may help the interpretation of muscle impedance signals for robotic orthoses control and provides physiological evidences that explain muscle resistivity variations observed in EIT images. It opens a new possibility to use these images, extracting information about muscle activation by means of digital processing, and use it to identify the operator's intention to control robotic orthoses. Proceeding this way it would be possible to access internal muscles that are not accessible by other methods such as EMG.

ACKNOWLEDGMENT

The authors would like to thank the Faculdade de Medicina Veterinária e Zootecnia da Universidade de São Paulo for lending the surgery room, the crew of veterinarians and anesthesiologists that collaborated in this experiment, and also to CNPq and CAPES for the financial support for this project.

REFERENCES

[1] P. J. Vauhkonen, *Image Reconstruction in Three-Dimensional Electrical Impedance Tomography*. PhD thesis, Department of Applied Physics, University of Kuopio, Finland, 2004.

[2] J. Victorino, J. Borges, V. Okamoto, G. Matos, M. Tucci, M. Caramez, H. Tanaka, F. S. Sipmann, D. Santos, C. Barbas, Carvalho, C.R.R., and M. Amato, "Imbalances in regional lung ventilation, a validation study on electrical impedance tomography," *Am. J. Crit. Care. Med.*, vol. 169, pp. 791–800, 2004.

[3] C. Gabriel, S. Gabriel, and E. Corthout, "The dielectric properties of biological tissues: I. literature survey," *Physics in Medicine and Biology*, vol. 41, no. 11, pp. 2231–2249., 1996.

[4] D. Miklavcic and F. X. Hart, "Electric properties of tissues," in *In Wiley Encyclopedia of Biomedical Engineering*, John Wiley & Sons, 2006.

[5] R. Pethig and D. B. Kell, "The passive electrical properties of biological systems: their significance in physiology, biophysics and biotechnology," *Physics in Medicine and Biology*, vol. 32, no. 8, pp. 933–970, 1987.

[6] A. Guyton and J. Hall, *Textbook of Medical Phisiology*. Elsevier Saunders, 1992.

[7] G. Radegran, "Limb and skeletal muscle blood flow measurements at rest and during exercise in human subjects," *Proceedings of the Nutrition Society*, vol. 58, no. 4, pp. 887–898, 1999.

[8] Y. Kawakami, Y. Ichinose, and T. Fukunaga, "Architectural and functional features of human triceps surae muscles during contraction," *Journal of Applied Physiology*, vol. 85, no. 2, pp. 398–404, 1998.

[9] B. M. Nigg and W. Herzog, *Biomechanics of the musculo-skeletal system*. Jonh Wiley and Sons, 2nd ed., 1999.

[10] J. Baskin and P. Paolin, "Volume change and pressure in muscle during contraction," *American Journal of Physiology*, vol. 213, no. 4, pp. 1025–1030, 1967.

[11] T. Goto, K. Tokumori, Y. Nakamura, M. Yahagi, K. Yuasa, K. Okamura, and S. Kanda, "Volume changes in human masticatory muscles between jaw closing and opening," *Journal of Dental Research*, vol. 81, no. 6, pp. 428–432, 2002.

[12] N. Place, T. Yamada, J. D. Bruton, and H. Westerblad, "Muscle fatigue: from observations in humans to underlying mechanisms studied in intact muscle fibers," *European Journal of Applied Physiology*, vol. 110, no. 1, pp. 1–15, 2010.

[13] R. Robergs, F. Ghiasvand, and D. Parker, "Biochemistry of exercise-induced metabolic acidosis," *Am J Physiol Regulatory Integrative Comp Physiol*, vol. 287, pp. R502–R516, 2004.

[14] R. Fitts, "Cellular mechanisms of muscle fatigue," *Physiological reviews*, vol. 74, no. 1, pp. 49–94, 1994.

[15] S. Rutkove, "Electrical impedance myography: background, current state, and future directions," *Muscle Nerve*, vol. 40, no. 6, pp. 936–946, 2009.

[16] C. Shiffman, H. Kashuri, and R. Aaron, "Electrical impedance myography at frequencies up to 2 mhz," *Physiological Measurement*, vol. 28, no. 6, pp. S345–S636, 2008.

[17] C. Shiffman, R. Aaron, and R. S.B., "Electrical impedance of muscle during isometric contraction," *Physiological Measurement*, vol. 24, no. 1, pp. 213–234, 2003.

[18] M. Ahad, P. Fogerson, RosenG.D., P. Narayanaswami, and S. Rutkove, "Electrical characteristics of rat skeletal muscle in immaturity, adulthood and after sciatic nerve injury, and their relation to muscle fiber size," *Physiological Measurement*, vol. 30, no. 12, pp. 1415–1427, 2009.

[19] T. Faes, H. van der Meij, J. de Munck, and R. Heethaar, "The electric resistivity of human tissues (100 hz–10 mhz): a meta-analysis of review studies," *Physiological measurement*, vol. 20, no. 4, pp. R1–R10, 1999.

[20] F. Gielen, W. W. de Jorge, and K. Boon, "Electrical conductivity of skeletal muscle tissue: experimental results from different muscles in vivo," *Medical and Biological Engineering and Computing*, vol. 22, pp. 569–577, 1984.

[21] R. Aaron, M. Huang, and C. Shiffman, "Anisotropy of human muscle via non-invasive impedance measurements," *Physics in Medicine and Biology*, vol. 42, no. 7, pp. 1245–1262, 1997.

[22] O. L. Silva, F. Moura, E. Camargo, S. T.B.R., and R. Lima, "Soleus and tibialis anterior activity detection using electrical impedance tomography," in *Proceedings of the XXIV Congress of International Society of Biomechanics – ISB*, (Natal, Brazil), 2013.

[23] T. Sousa, F. Moura, I. Hoffmann, E. Camargo, R. Lima, A. Martins, D. Fantoni, and C. Biasi, "In vivo admitivity measurements for regularizations in electrical impedance tomography," in *Proceedings of COBEM 2011, 21st International Congress of Mechanical Engineering*, (Natal, Brasil), October 24–28 2011.